JMEPEG (1998) 7:393-401

Mechanical Behavior of Al-Al_2O_3 MMC Manufactured by PM Techniques Part I—Scheme I Processing Parameters

A.A. Mazen and A.Y. Ahmed

(Submitted 18 June 1997; in revised form 29 January 1998)

Metal matrix composites (MMC) were manufactured using hot pressing followed by hot extrusion of aluminum (Al) powder reinforced by alumina (Al_2O_3) particles. Under tensile as well as compressive loads, a strength improvement of 64 to 100% compared to the matrix material strength was obtained. The percent elongation to fracture ranged from 20 to 30%, which indicates good ductility as compared to the ductility of MMC manufactured by other techniques. Optical as well as scanning electron microscopy (SEM) examinations were used for characterization of the material microstructure and fracture behavior. Porosity retained in the microstructure was very limited in the case of pure aluminum billets. Microstructural examination revealed uniform distribution of Al_2O_3 particles in the Al-matrix. Under tensile loads, voids opened by decohesion between the matrix and reinforcement. Such behavior led to a decrease in strength properties of the MMC as a function of reinforcement volume fraction. The fracture surface is dominated by the ductile fracture features, that is, dimples. Voids were found to initiate at retained porosity sites at the Al/Al_2O_3 interface or in the matrix close to the interface due to stress concentration. The SEM revealed the formation of a complex fine subgrain structure. Such a polygonized structure is a major source of strengthening.

Keywords fractography, mechanical behavior, metal matrix composites, microstructures, powder metallurgy

1. Introduction

Metal matrix composites (MMC) are manufactured using different techniques. These techniques could be classified as (a) liquid-phase (casting) processes, for example, squeeze casting (Ref 1-4), vacuum infiltration (Ref 5-6), pressureless infiltration (Ref 7-8), and dispersion methods (Ref 9), (b) solid state processes, for example, powder metallurgy (PM) techniques with variations in the processing steps, that is, use of hot sintering, cold sintering, hot pressing, dynamic compaction (Ref 2, 10), and (c) liquid-solid processing, for example, compocasting, semisolid forming (Ref 11).

The limitations of the first and third groups arise from difficulties in mixing the two phases thoroughly, difficult determination of critical temperature for infiltration, problems due to fluidity and/or wettability at matrix-reinforcement interface, as well as harmful reactions at the interface.

Powder metallurgy (PM) techniques are used extensively in manufacturing particulate MMC. Using these techniques, the matrix as well as the reinforcement are used in the form of powder. The powders are thoroughly mixed in the solid state; then they are manufactured into billets using vacuum hot pressing or degassing followed by hot pressing and hot extrusion.

Several advantages could be achieved using this method. Homogeneity of the mixture is well controlled. The produced composite inherits all the advantages of the rapidly solidified powdered metals, and the component is produced in near net-shape dimensions.

Of all metals, aluminum is used most commonly as a matrix for MMC. The light weight of aluminum allows the production of high strength to weight ratio materials. The major obstacle in the processing of aluminum using PM methods is the oxide and hydroxide films coating the powder (Ref 12). Aluminum oxide as well as aluminum hydroxide layers affect the bonding and mechanical behavior of materials made from powdered aluminum. Usually, sophisticated techniques of degassing or vacuum pressing are used to produce higher mechanical strengths. However, these techniques add limitations to the size and geometry of the produced billet. Thus, to reach final shape, extensive machining might be needed. This cancels a major advantage of PM techniques, that is, producing near net-shape components.

2. Processing Parameters

Many parameters control the mechanical behavior of metal matrix composites manufactured by PM techniques. These parameters could be classified as intrinsic and extrinsic parameters. The intrinsic parameters include particle size, particle size distribution of both matrix and reinforcement powders, reactivity and affinity of matrix and reinforcement particles to each other, which controls the formation of an interface, its depth and strength, and so on.

Extrinsic parameters are those related to processing variables. These include compaction parameters: uniaxial or multiaxial compaction, compaction stress, compaction temperature, compaction rate, and time at maximum load.

A.A. Mazen and **A.Y. Ahmed,** Mechanical Engineering Dept., The American University in Cairo, Egypt.

The results of an experimental study on the mechanical behavior of Al-Al_2O_3 MMC manufactured by PM techniques is presented. Two processing schemes are used in manufacturing the specimens. In Scheme I, the compaction parameters consisted of compaction stress of 74 MPa and compaction temperature of 723 K applied for 4 h, followed by hot extrusion. In Scheme II, the compaction parameters were a compaction stress of 157 MPa, a compaction temperature of 873 K applied for 3 h, followed by hot extrusion. The results of the first scheme are presented here.

3. Experimental Program

3.1 Specimen Fabrication

Preweighed pure alumina powder (Al_2O_3) was mixed as a reinforcement with pure aluminum (Al) powder as matrix. Through the use of a mechanical mixer, the two powders were thoroughly mixed to achieve homogenization.

Four different compositions were prepared, that is, Al-0wt%Al_2O_3, Al-2.5wt%Al_2O_3, Al-5wt%Al_2O_3, and Al-10wt%Al_2O_3.

The Al-Al_2O_3 powder mixture was then hot pressed using the hot-pressing setup shown in Fig. 1, using a compaction pressure of 74 MPa on the 24 mm diameter billets. Pressing was done at 723 K. The temperature was maintained for 4 h at the maximum compaction pressure.

The hot-pressed billets were then hot extruded at 723 K with an extrusion ratio of 5. The extruded rods were used as raw stock out of which specimens for different test were machined.

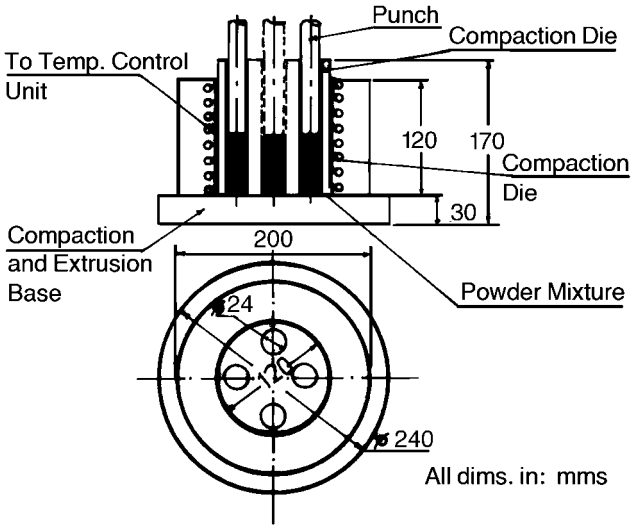

Fig. 1 Hot pressing and extrusion setup

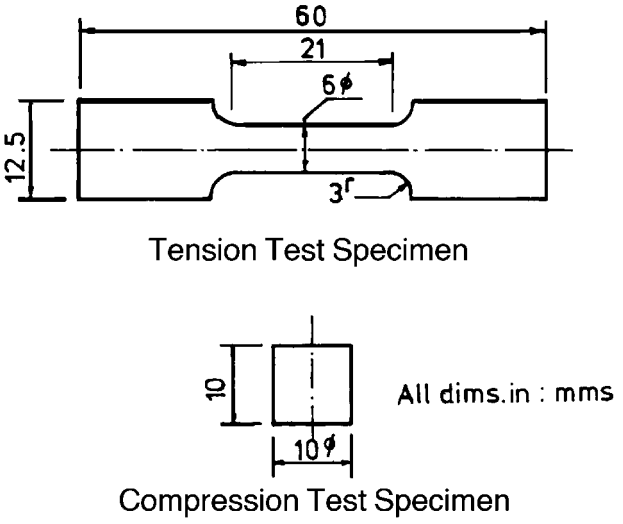

Fig. 2 Test specimen geometry

3.2 Tension Testing

Tension testing at room temperature was conducted in a universal testing machine using an average strain rate of 10^{-3} s^{-1} along the 15 mm gage length. The specimen geometry is shown in Fig. 2.

3.3 Compression Testing

Cylindrical specimens of aspect ratio *h*o/*d*o = 1.0, where *h*o and *d*o are the initial height and diameter of the specimen, respectively, were tested under conditions of no friction at specimen/compression platen interface. The crosshead speed was adjusted to give an average strain rate of 10^{-3} s^{-1} across the specimen height. The test was terminated after considerable reduction in height (corresponding to a strain of 60% or more) or at the observation of the first surface fracture. Specimens that showed fracture failed by shearing, and the fracture was inclined at an angle of 45° to the load axis.

3.4 Microstructural and Fracture Surface Examinations

Specimens for different conditions were prepared, and their microstructures were examined in an optical microscope.

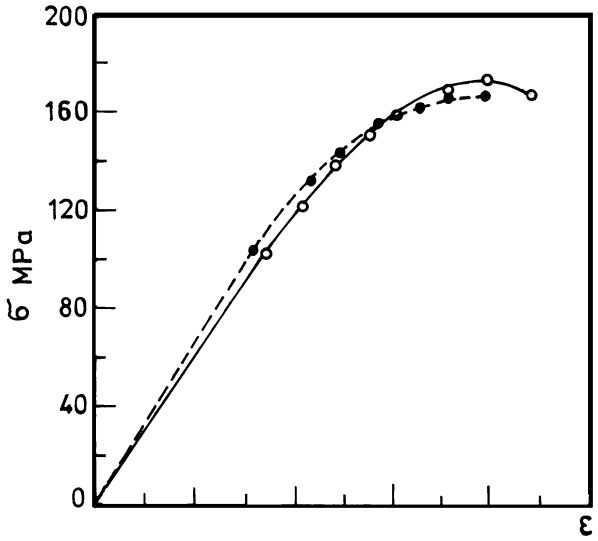

Fig. 3 Stress-strain curves for Al-0wt%Al_2O_3 (two different batches)

Scanning electron microscopy (SEM) was used to examine and analyze the fracture mechanism in the tension test specimens.

4. Analysis and Discussion of Results

4.1 Mechanical Characteristics of Unreinforced PM Aluminum

Figure 3 shows the tension stress-strain curves of two specimens made of the same chemical composition, Al-0wt%Al_2O_3, and manufactured using the same processing parameters. The two curves are almost identical, and the variations are within a reasonably narrow range. Table 1 summarizes the tensile mechanical parameters for commercially pure aluminum manufactured using different techniques as given in corresponding references. The material showed significant improvement in strength and ductility compared to these materials. For example, using PM techniques, Arsenault and Wu (Ref 13) obtained a yield strength of 37.3 MPa, whereas the yield strength presently achieved is 104 MPa, an improvement of 178%. The ultimate tensile strength showed an improvement of 100%. The ductility expressed in terms of percent elongation to fracture also improved as compared to pure aluminum manufactured by other techniques (Ref 14-16). However, aluminum processed by casting techniques gave higher ductilities (Ref 17-19). The increase in ductility and strength parameters could be attributed to the small grain size, which is characteristic of materials produced by PM techniques. As seen in SEM fractographs, the microstructure consists of small grains and smaller subgrain structure. Such a structure could lead to generation of high dislocation density during deformation and thus act as an efficient barrier to dislocation motion. Arsenault et al. (Ref 20) showed that when high dislocation densities and small subgrain sizes develop in pure aluminum, its strength could reach levels comparable to that of Al-20wt%SiC composites.

4.2 Tensile Deformation Behavior of Al-Al_2O_3 Composites

Figure 4 shows the tensile stress-strain curves of Al-Al_2O_3 MMC materials as a function of the weight percent reinforcement. The yield and ultimate strength were substantially affected by the addition of Al_2O_3 particles. As shown in Table 2, the yield strength of the composites, except for Al-2.5wt%Al_2O_3, demonstrated improvement over that of unreinforced aluminum. Such an increase in yield strength could be attributed to the presence of reinforcing particles, which constrain the plastic flow of the matrix material. A maximum improvement of 20% over the matrix was obtained for Al-10wt%Al_2O_3.

Table 1 Tensile properties of commercially pure aluminum produced by different techniques

Manufacturing technique	Yield stress, MPa	Tensile strength, MPa	Elongation, %	Reference
Casting	29.0	40.0	37.0	14
Casting	32.0	81.0	42.0	15
Casting	35.0	90.0	45.0	16
Casting	25.6	93.0	…	17
Squeeze Casting	56.0	84.0	19.3	18
Spray roll	…	127.0	22.0	19
Vacuum infiltration	…	72.0	22.8	20
PM	37.0	85.6	…	21
PM	103.8	171.0	29.4	Present work

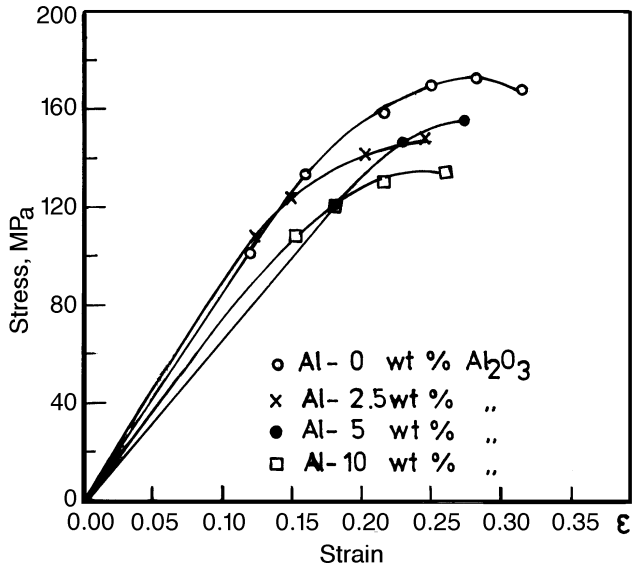

Fig. 4 Tensile stress-strain curves for Al-Al_2O_3 MMC

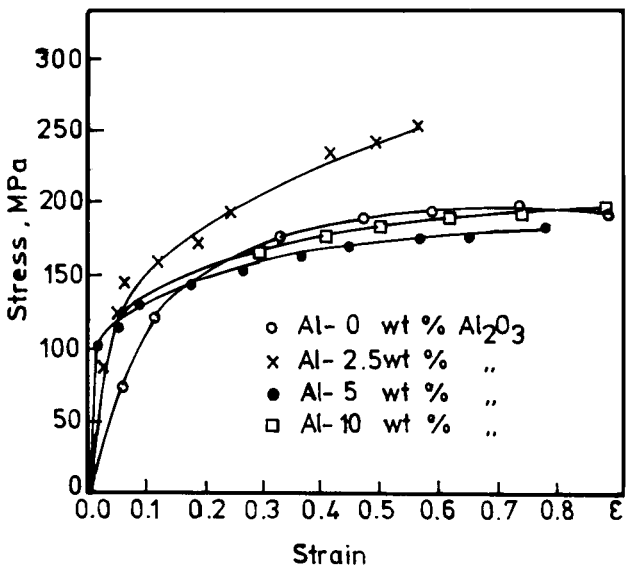

Fig. 5 Compressive stress-strain curves for Al-Al_2O_3 MMC

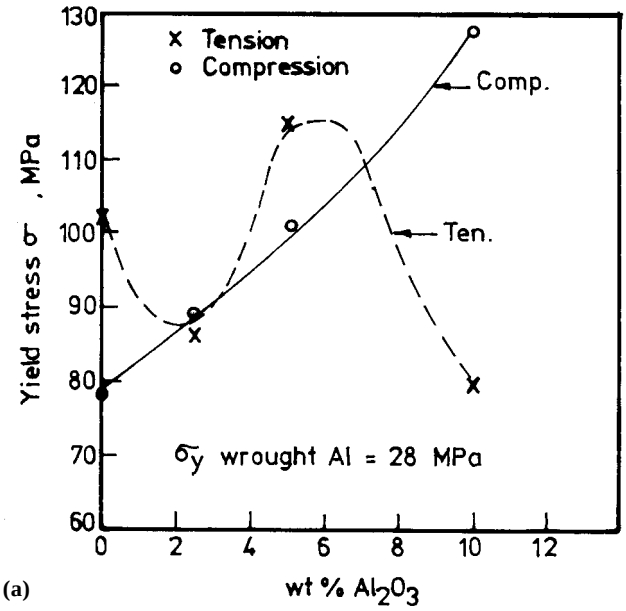

(a)

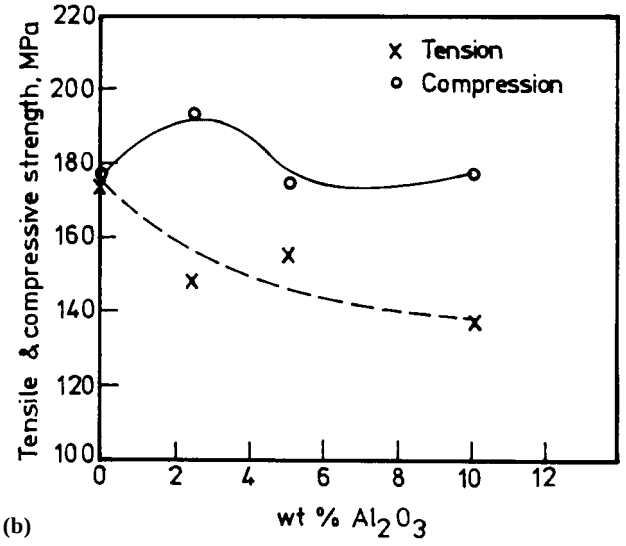

(b)

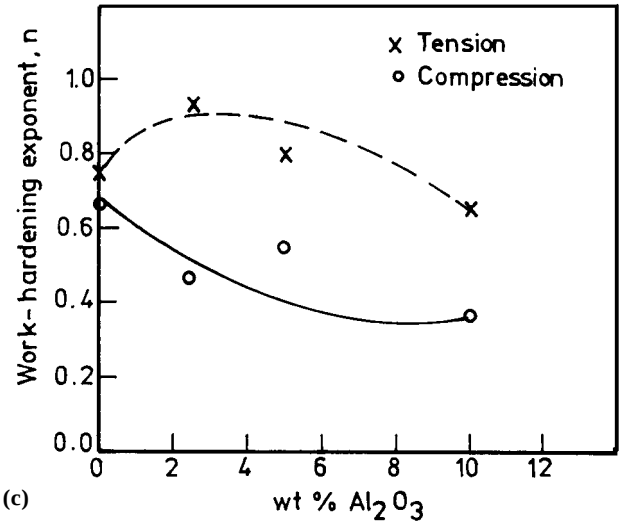

(c)

Fig. 6 Variation of deformation characteristics with weight percent Al_2O_3

In contrast, the tensile strength of the MMC continued to decrease as more Al_2O_3 particles were added to the matrix. Decreases of 13% for Al-2.5wt%Al_2O_3 and 20% for the other two compositions were observed. Two factors affect the magnitude of the tensile strength; they are the homogeneity of distribution of reinforcement particles in the matrix and the bond strength developed between the two phases. Optical microscopy and SEM revealed the presence of porosity and particle-rich areas in the matrix. This nonuniformity of particle distribution is usual in MMC materials. It affects the stress and strain distribution and develops triaxial stresses in the matrix. As a result, large stress gradients are generated locally in the matrix, and these regions are potential sites for failure (Ref 21-23).

The other factor that affects the tensile strength of MMC materials is the bond strength between the matrix and the reinforcement particles. It was observed during SEM fractographic examination that some alumina particles are totally debonded. This indicates weak bond strength and could be explained in view of the large difference between the melting points of Al and Al_2O_3. In liquid phase processing of MMC, wettability, which enhances the bond strength, is achieved only at high processing temperatures (>1173 K) (Ref 1). In solid state Al-Al_2O_3 MMC, a strong interfacial bond is possible only above 918 K (Ref 24). Also, the absence of alloying elements in the matrix contributed to the weak interfacial bond. Hosking et al. (Ref 25) attributed the decrease in tensile strength of Al-Al_2O_3 MMC compared to that of the unreinforced matrix to the absence of degassing in their processing of the composite. Degassing was not used in processing of the specimens to simplify the process. Thus, this could be another factor that explains the decrease in the tensile strength of the composite. However, a comparison of Tables 2 and 1 shows that the lowest tensile strength obtained is higher than the tensile strength obtained for MMC manufactured by all other techniques. For example, an improvement of approximately 59% is obtained if the tensile strength of Al-10wt%Al_2O_3 of the present work is compared to that of Ref 14.

4.3 Compressive Deformation Behavior of Al-Al_2O_3 MMC

Figure 5 shows the stress strain curves under compressive loads. The yield stress of the unreinforced matrix (i.e., pure Al) was found to be 78 MPa. This represents an improvement of 105% compared to the values published in Ref 14. The yield strength continued to increase as Al_2O_3 particles were added to the matrix. At 10 wt% Al_2O_3, the yield stress reached 128 MPa, an improvement of 64% over the yield stress of unreinforced matrix.

The improvement in yield strength indicates the effectiveness of Al_2O_3 particle in hindering the motion of dislocations. Such a role is enhanced by the densification processes that occur under compressive loads (Ref 26). These processes consist of two elements: densification due to compressive deformation of the matrix grains and densification due to closure of any pores at matrix particle interfaces.

The compressive strength, σ_c, for the tested specimens was taken arbitrarily as the stress corresponding to a strain of 50%. Large improvement in σ_c was observed for Al-2.5wt%Al_2O_3 as compared to unreinforced Al. However, for the other

compositions, the composite showed slight reduction in the compressive strength. Again, this reduction could be attributed to microstructural features such as clusters of reinforcing particles and lack of perfect bond between the two phases. Such features lead to softening of the material under compressive loads. This also explains the large ductilities observed under compressive loads, which reached ~85% in the case of Al-10wt%Al_2O_3.

4.4 Hardening Behavior of Al-Al_2O_3 MMC

Figure 6(c) shows the variation of the work-hardening exponent, *n*, in the power law, $\sigma = K\varepsilon^n$, with the type of loading as a function of the weight percent alumina. Under tensile as well as under compressive loads, *n*-values were found to be quite different from those of ingot aluminum. Ingot commercially pure aluminum has an *n* of 0.25 (Ref 27). In the present work, unreinforced aluminum had an *n* of 0.65 under tension and an *n* of 0.75 under compression. The exponent *n* varies with the type of loading and with variations in material composition. The *n*-values obtained under tensile loads are always higher than those under compressive loads. Such high values of *n* are characteristic of PM materials with retained porosity. It reflects the effects of the difference between macroscopic and microscopic deformations. While macroscopic deformations might be low, microscopic deformations could be appreciable and accompanied by significant hardening (Ref 28).

4.2 Microstructural Analysis

Figures 7 through 9 show the micrographs of specimens of different Al_2O_3 weight fractions under different loading conditions. All micrographs were taken in the as-polished and etched condition at a magnification of 188×. Figures 7(a-d) show the microstructures of the material before testing, that is, hot pressed and extruded.

Figure 7(a) (Al-0wt%Al_2O_3) shows some retained porosity in the microstructure, which appear as little black spots scattered throughout the micrograph. Fig. 7(b-d) show that the alumina particles are uniformly distributed in the aluminum matrix. Clusters of particles were observed during SEM examinations. Thus, it is believed that each of the spherical

Table 2 Tensile properties of Al-Al_2O_3 MMC

Technique	Composition	Yield stress, MPa	Tensile strength, MPa	Elongation, %	Reference
Casting	Al-20wt%Al_2O_3	116	142	1.10	14
	Al-2.2 (Al_2O_3-Mg0)	48	92	24.0	15
PM	Al-2.5wt%Al_2O_3	87.5	148.8	24.7	Present work
	Al-5wt%Al_2O_3	115.5	155.0	27.0	Present work
	Al-10wt%Al_2O_3	124.3	136.3	26.7	Present work

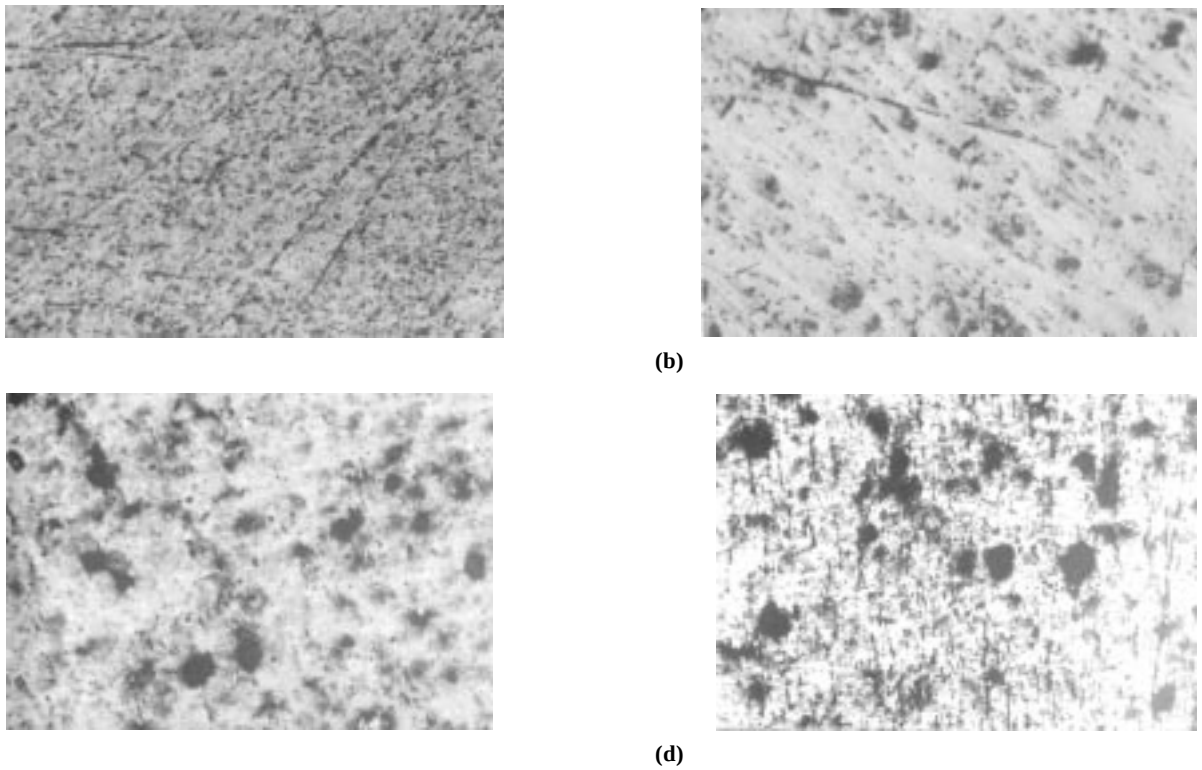

Fig. 7 Microstructures of material before testing (188×). (a) Al-0wt%Al_2O_3, (b) Al-2.5wt%Al_2O_3, (c) Al-5wt%Al_2O_3, and (d) Al-10wt%Al_2O_3

black areas in Fig. 7(b-d) consist of clusters of alumina particles surrounded by an interface of porous aluminum matrix.

Figures 8(a-d) show the microstructures of the different compositions after compression testing. It is clear that compressive loads have significant effects on the morphology of the reinforcement particles. While these particles appear as circular cross-sections before testing, they become flattened and elongated after compressive loads. This morphology change is the direct result of shearing strains experienced by the matrix during deformation. Due to mechanical bond and strong interlocking between the particles and the matrix, that is, generated by severe friction at high temperature during processing, the particles followed the same deformation pattern dictated by the matrix. The alumina particles embedded in the matrix acted as stress concentration sites as well as strain localization sites. This explains the reduction in compressive strength of the Al-Al_2O_3 MMC as compared to that of the unreinforced matrix.

Figures 9(a-d) show micrographs of specimens tested under tensile loads. Due to tensile strains, the matrix-particle interface opens, creating voids. This helps in accelerating the fracture process by reducing it from a three-stage process, that is, initiation, propagation, and growth into a two-stage process, that is, propagation and growth.

4.3 Fracture Mechanisms in Al-Al_2O_3 PM MMC

Figures 10(a-d) show the SEM fractographs taken for specimens of different Al_2O_3 content. The main mechanism of fracture is the ductile mode of void initiation, growth, and coalescence. Figure 10(a) shows the fractograph of pure PM aluminum (Al-0%Al_2O_3). The fractograph is dominated by dimples of different sizes. Figures 10(b) and 10(d) clearly show the clusters of alumina particles in the matrix (indicated by arrows on the fractograph). Porosity can be observed between these particles and at a particle/matrix interface. Voids initiate first at this retained porosity. Once these voids grew, strain localization caused more void initiation at the weakest interparticle bonds. Coalescence of these voids lead to eventual fracture. The fractographs show that the microstructure consists of subgrain structure in larger grains. Thick ligaments of the matrix material appear to have bound this fine subgrain structure, which provides a strong barrier to dislocation motion due to its entanglement and complexity. This observation explains the remarkable improvement in yield strength of PM aluminum over conventional ingot aluminum. Such polygonized substructure usually develops during hot working (Ref 29). The use of powdered metal coupled with the processing sequence of hot pressing followed by hot extrusion lead to the formation of

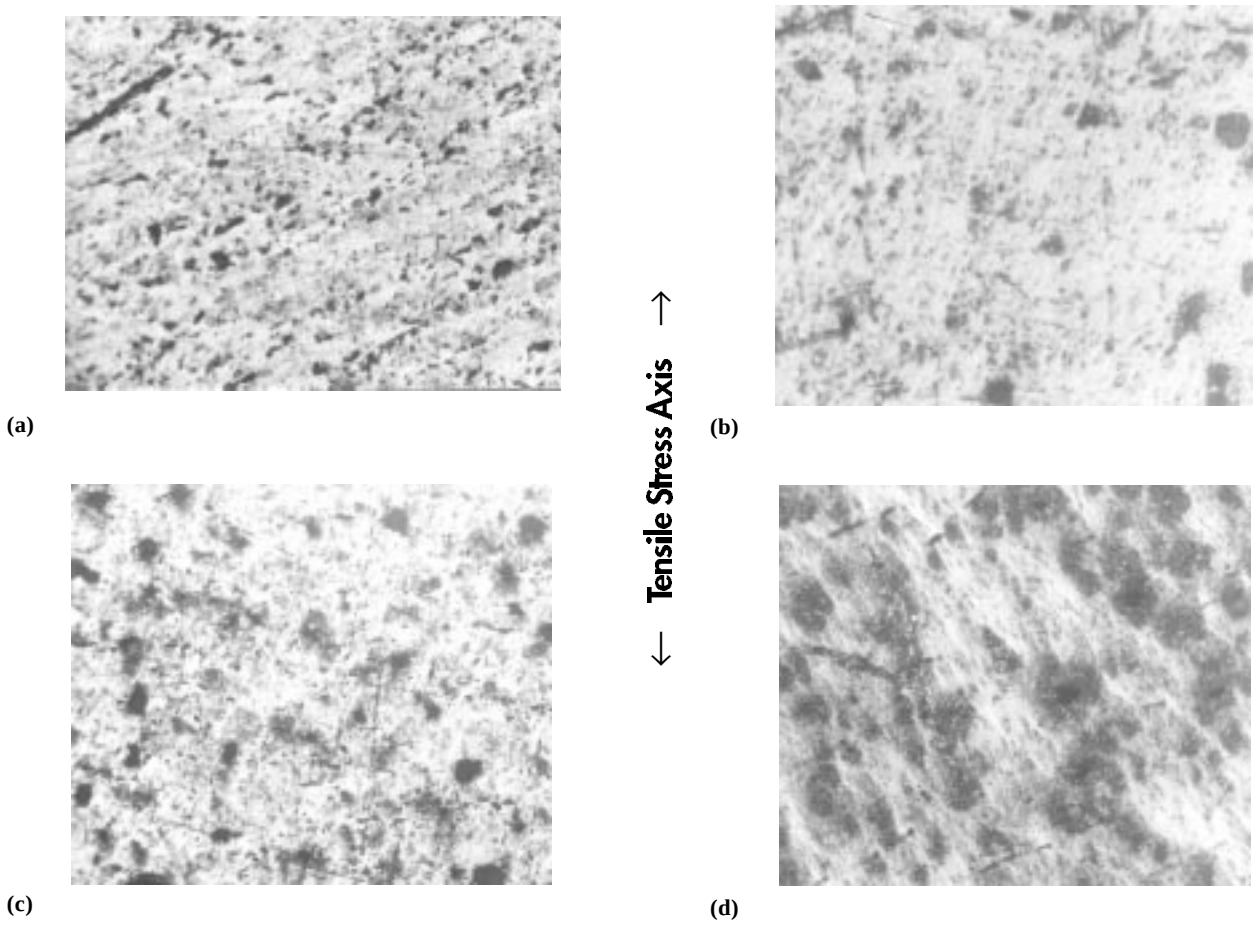

Fig. 8 Microstructures of tensile deformed specimens (188×). (a) Al-0wt%Al_2O_3, (b) Al-2.5wt%Al_2O_3, (c) Al-5wt%Al_2O_3, and (d) Al-10wt%Al_2O_3

such polygonized substructures. Figure 10(d) shows more clearly the thick ligaments surrounding the fine subgrain structure. As the Al_2O_3 weight percent increases (Fig. 10b-d), more Al_2O_3 particles exist as unbonded free particles in the matrix. Such behavior explains the reduction in strength accompanying the increase in Al_2O_30 weight percent. Figure 11 shows an Al_2O_3 particle unbonded to the aluminum matrix. It is clear that microvoids initiated at the boundaries of the particle. Figure 12 shows a view of the thick ligament mentioned above. Voids initiate in this case at the retained porosity sites.

5. Conclusions

- Hot pressing followed by hot extrusion without complicated techniques of vacuum pressing or degassing is capable of producing strong microstructures in aluminum matrix composites by disrupting the oxide and hydroxide layers coating aluminum powder particles. Processing parameters, such as temperature and pressure, play a key role in determining final mechanical properties.
- Under tensile and compressive loads, a strength improvement of 64 to 100% compared to the matrix material strength was obtained. Such strength improvement was attributed to the formation of fine subgrain structure as revealed by the SEM fractographs.
- Al-Al_2O_3 MMC manufactured by PM techniques exhibited considerable ductility (elongation to fracture of up to 31%), which is an advantage of this technique over other techniques of MMC manufacturing.
- The stress-strain data were found to fit nicely with the power law, $\sigma = K\varepsilon^n$; however, the work-hardening exponents, n, have high magnitudes, characteristic of PM materials.
- Microstructural examination of specimens of different Al_2O_3 weight percent revealed the presence of retained po
- Al_2O_3 particles were observed to be uniformly distributed throughout the microstructure. The morphology of these particles is affected by the compressive loads to become flattened and elongated. Under tensile loads, the matrix adjacent to these particles opened by decohesion. This is a major source for initiation of voids in the fracture process.
- SEM fractographs revealed that the main fracture mechanism in Al-Al_2O_3 MMC is the ductile mode of void initiation, growth, and coalescence. Voids initiated at Al-Al_2O_3 interfacial sites or the porosity retained in the aluminum matrix.
- This research will be extended to examine the effects of different processing parameters on the mechanical behavior of Al-Al_2O_3 MMC.

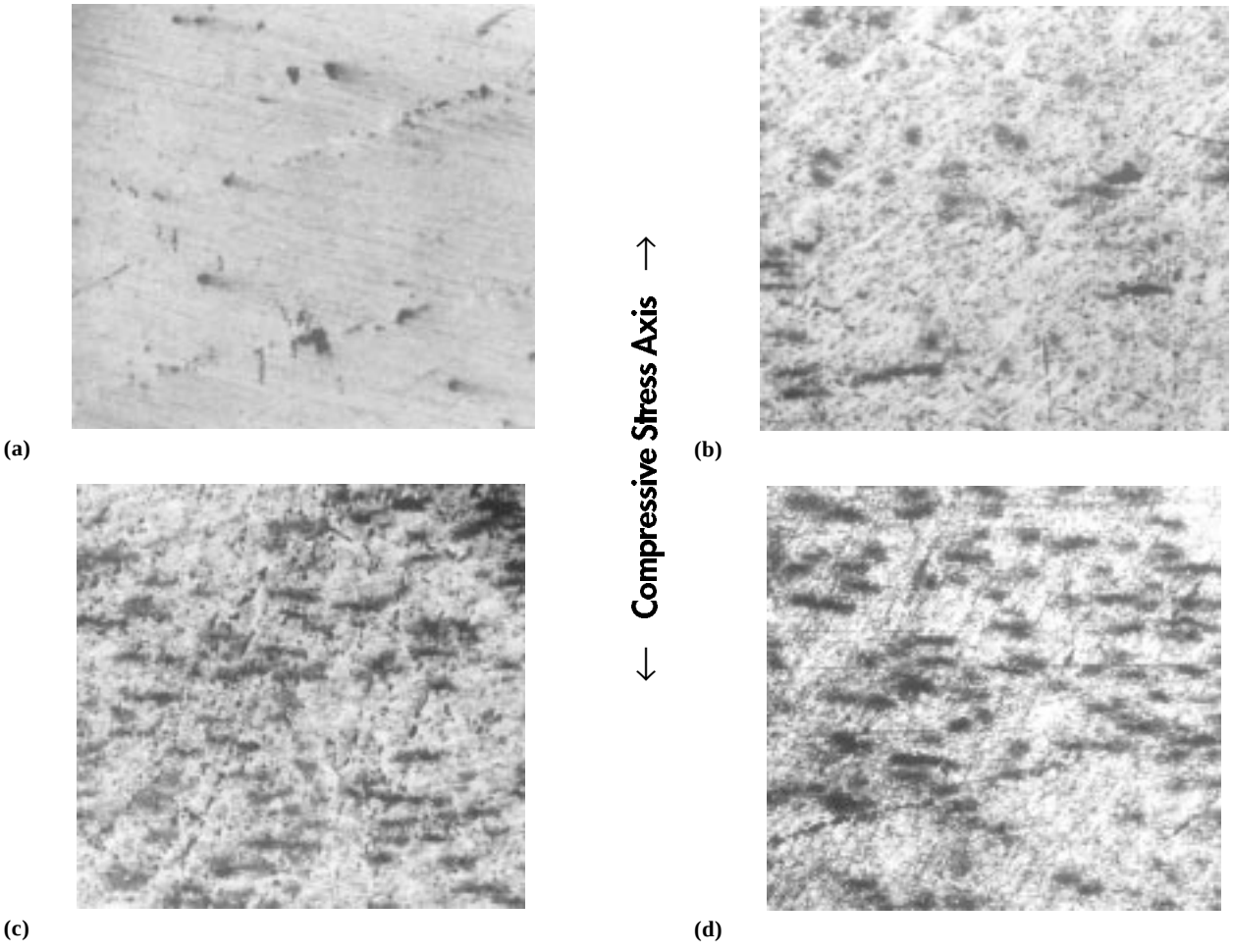

Fig. 9 Microstructures of compressively deformed specimens (188×). (a) Al-0wt%Al_2O_3, (b) Al-2.5wt%Al_2O_3, (c) Al-5wt%Al_2O_3, and (d) Al-10wt%Al_2O_3

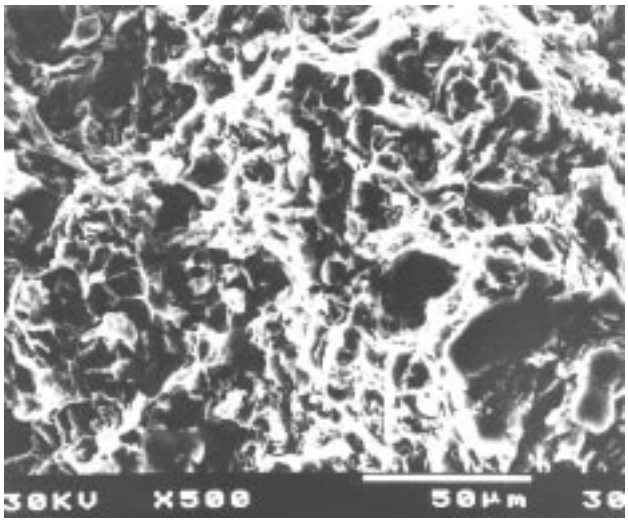

(a)

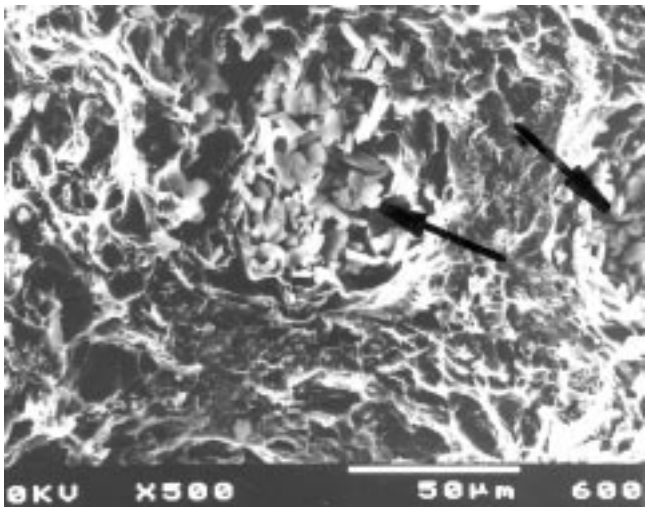

(b)

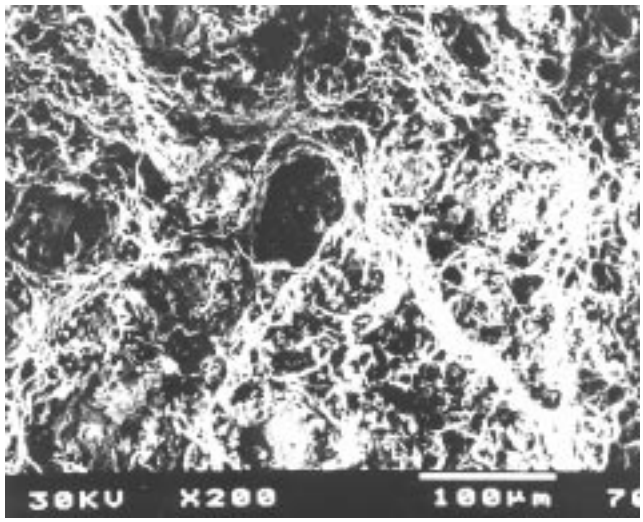

(c)

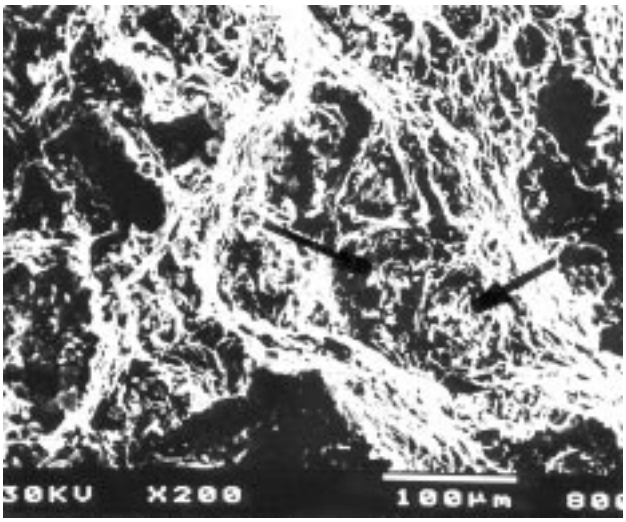

(d)

Fig. 10 SEM fractographs. (a) Al-0wt%Al_2O_3, (b) Al-2.5wt%Al_2O_3, (c) Al-5wt%Al_2O_3, and (d) Al-10wt%Al_2O_3

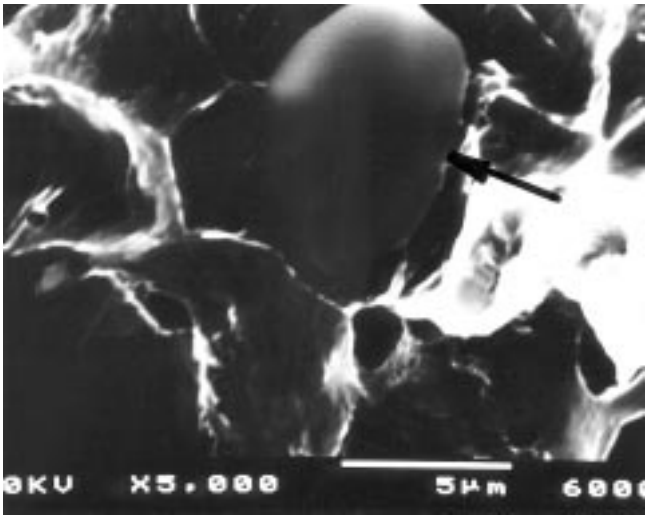

Fig. 11 Unbonded Al_2O_3 particle in Al-matrix

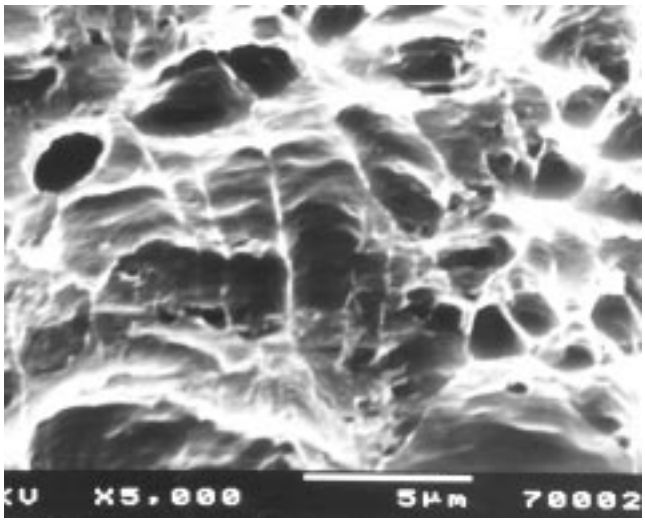

Fig. 12 Thick ligament of strongly bonded Al-matrix

References

1. I.A. Ibrahim, F.A. Mohamed, and E.J. Lavernia, Particulate Reinforced Metal Matrix Composites, a Review, *J. Mater. Sci.*, Vol 26, 1991, p 1137-1156
2. A.W. Urquhart, Molten Metals Sire MMC and CMC's, *Adv. Mater. Process.*, ASM International, Materials Park, OH, Vol 7, 1991
3. E.M. Klier, A. Montensen, J.A. Cornie, and M.C. Flemings, Fabrication of Cast Particle-Reinforced Metal Via Pressure Infiltration, *J. Mater. Sci.*, Vol 26, 1991, p 2519
4. J. Singh, S.K. Goel, V.N.S. Mathur, and M.L. Kapoor, Elevated Temperature Tensile Properties of Squeeze-Cast Al-Al_2O_3-MgO Particulate MMC's up to 573 K, *J. Mater. Sci.*, Vol 26, 1991, p 2750
5. J. Yang and D.D.L. Chung, Casting Particulate and Fibrous MMC's by Vacuum Infiltration of a Liquid Metal under an Inert Gas Pressure, *J. Mater. Sci.*, Vol 24, 1989, p 3605
6. J.M. Chiou and D.D.L. Chung, Characterization of MMC's Fabricated by Vacuum Infiltration of a Liquid Metal under an Inert Gas Pressure, *J. Mater. Sci.*, Vol 26, 1991, p 2583
7. B.D. Agarwal and L. Braatman, *Analysis and Performance of Fiber Composites*, John Wiley & Sons Ltd., 1990
8. A.M. Assar and M. Nimr, Fabrication of MMC by Infiltration Process: Part 1: Modeling of Hydrodynamic and Thermal Behavior, *J. Compos. Mater.*, Vol 28 (No. 15), 1994, p 1480
9. D.G.C. Syu and A.K. Ghosh, The Effect of Temperature on the Fracture Mechanism in 2014 Al/15 vol%Al_2O_3 Composite, *Mater. Sci. Eng., A*, Vol 184, 1994, p 27-35
10. Y.B. Liu, S.C. Lim, L. Lu, and M.O. Lai, Recent Development in the Fabrication of Metal Matrix Particulate Composites using Powder Metallurgy Techniques, *J. Mater. Sci.*, Vol 29, 1994, p 1999-2007
11. K. Manaba and S. Sumio, *Proc. of Second Int. Conf. on Semi-Solid Alloys and Composites*, 1992, p 382
12. Y.W. Kim, W.M. Griffith, and H.H. Fors, "The Breakup and Distribution of Surface Oxides Through Processing of PM Aluminum Alloy 7091," (Philadelphia, PA), Oct 1983, ASM Metals Congress
13. R.J. Arsenault and S.B. Wu, A Comparison of PM vs Melted SiC/Al Composites, *Scr. Metall.*, Vol 22, 1988, p 767
14. M.G. McKimpson and T.E. Scott, Processing and Properties of MMC's containing Discontinuous Reinforcement, *Mater. Sci., Eng.*, Vol A107, 1989, p 93-106
15. M.K. Aghajanian, M.A. Rocazella, J.T. Burke, and S.D. Keck, The Fabrication of MMCs by a Pressureless Infiltration Technique, *J. Mater. Sci.*, Vol 26, 1991, p 447
16. S.-W. Lai and D.D.L. Chung, Super High-Temperature Resistance of Aluminum Nitride Particle-Reinforced Aluminum Compared to Silicon Carbide or Alumina Particle-Reinforced Aluminum, *J. Mater. Sci.*, Vol 29, 1994, p 6181
17. S.J. Harris, Cast Metal Matrix Composites, *Mater. Sci. Technol.*, Vol 4, 1998, p 231
18. N.I. Abdul-Latif, A.I. Khedar, and S.K. Goel, Microstructure and Mechanical Properties of Al-Al_2O_3-MgO Cast Particulate Composites, *J. Mater. Sci.*, Vol 22, 1987, p 466-472
19. S. Kalpakjian, *Manufacturing Processes for Engineering Materials*, 3rd ed., Addison-Wesley, 1997
20. R.J. Arsenault, L. Wang, and C.R. Feng, Strengthening of Composites Due to Microstructured Changes in the Matrix, *Acta Metall.*, Vol 39, 1991, p 47-57
21. S.F. Corbin and D.S. Wikinson, Effect of Temperature on the Mechanical Behaviour of a SiC Particulate Reinforced Al-Alloy, *Proc. of Inter. Symposium on Advances in Processing of Ceramics and MMC*, H. Mostaghaci, Ed., Helix, Aug 1989, p 401-411
22. Z. Wang, T.K. Chen, and D.J. Lloyd, Stress Distribution in Particulate-Reinforced MMC Subjected to External Load, *Metall. Trans. A*, Vol 24, 1993, p 197
23. T. Christman, A. Needleman, and S. Suresh, An Experimental and Numerical Study of Deformation in Metal-Ceramic Composites, *Acta Metall. Mater.*, Vol 37, 1989, p 3029-3050
24. D.-G.C. Syu and A.K. Ghosh, Forging Limited for an Aluminum Matrix Composite: Part II Analysis, *Metall. Mater. Trans. A*, Vol 25, 1994, p 2039
25. F.M. Hosking, F.F. Portillo, R. Wunderlin, and R. Mehrabian, Composites of Aluminum Alloys: Fabrication and Wear Behaviour, *J. Mater. Sci.*, Vol 17, 1982, p 477
26. H.A. Kuhn, *Powder Metallurgy Processing*, H.A. Kuhn and A. Lawley, Ed., Academic Press, 1978, p 99
27. R.M. Cadell, *Deformation and Fracture of Solids*, Prentice-Hall, Inc., 1980, p 102
28. A.A. Mazen, "Plastic Flow Behavior of Porous Metals," Ph.D. thesis, UCLA, 1989
29. P. Olla and P.F. Virdis, High Temperature Deformation of a Commercial Aluminum Alloy, *Metall. Trans. A*, Vol 18, Feb 1987, p 293-301